THREE-DIMENSIONAL VISCOUS FLOWS IN FURNACE CHAMBERS

V. B. Dovzhik and V. K. Migai

UDC 532.516.5:662.9

A method is proposed for calculating isothermal flows in channels of complex configuration, for the example of a vortex furnace chamber.

Current furnace technology is distinguished by great diversity of aerodynamic schemes: As well as the traditional opposed grouping of vortex or direct-furnace burners and the tangential grouping, other types employed are the furnaces designed by the I. I. Polzunov Central Scientific-Research Institute for the Planning and Design of Boilers and Turbines (CSIPDBT) and the Leningrad Polytechnic Institute, cyclone furnaces, multifaceted annular furnaces, and furnaces with plane-flame burners. This diversity of aerodynamic schemes is not by chance, since aerodynamics is one of the factors determining the combustion and heat-transfer processes in furnaces. Therefore, in developing new designs of boiler units, the study of gas-flow aerodynamics inside furnace chambers is of great importance. To date, this question has basically been approached by numerical modeling. However, the development of methods of computational hydrodynamics and progress in computer technology permits the use of mathematical methods of modeling the aerodynamic processes together with physical methods. The promise of this approach is indisputable, since a successful mathematical model may permit operative change in the boundary conditions and configuration of the design, and subsequently the consideration of heat and mass transfer in the boiler units, together with aerodynamics.

However, mathematical modeling of furnace processes encounters large but not insuperable difficulties associated with the complexity of the phenomena being modeled and the imperfection of the computer technology employed (inadequate speed and memory capacity). Flow in furnace chambers is spatially complex, and thus the problems to be solved are unconditionally three-dimensional. Only certain forms of flow [1] may be described in a two-dimensional coordinate system, offering the possibility of including the model of turbulence and combustion in consideration. In solving three-dimensional problems, on the one hand, the range of problems considered must be restricted and, on the other, coarse grids must be used.

In the present work, in constructing a numerical method of investigation, it is taken into account that the maximum velocities in the furnaces are no greater than 100 m/sec. At temperatures of around 1800 K, this corresponds to a Mach number $M \leq 0.12$. At such values of M, the liquid may be regarded as incompressible.

In flame ignition of fuel and oxidizing agent, jets are introduced in the furnace volume and, interacting with one another and with the boundary surfaces, mix well and form a single flow; this allows the flow to be regarded as isothermal, in the first approximation.

Turbulent motion of the incompressible liquid may be described by the Reynolds equations. If they are closed using the Boussinesq hypothesis and the assumption that the turbulent viscosity is constant and much larger than the molecular viscosity, these equations reduce to the Navier–Stokes equations. As well as the continuity equation, the following system is obtained here

$$\sum_{k=1}^{N}\left(u_k\frac{\partial u_i}{\partial x_k}-\frac{1}{\mathrm{Re}_{\mathrm{ef}}}\frac{\partial^2 u_i}{\partial x_k^2}\right)+\frac{\partial P}{\partial x_i}=0,\ i=1,\ \ldots,\ N,\ \sum_{k=1}^{N}\frac{\partial u_k}{\partial x_k}=0. \tag{1}$$

The assumption of constant turbulent viscosity is fairly rough. However, taking account of the lack of information on turbulent viscosity for such flows, the three-dimensionality of

Scientific-Design Department, I. I. Polzunov Central Scientific-Research Isntitute for the Planning and Design of Boilers and Turbines, Leningrad. Translated from Inzhenerno-Fizicheskii Zhurnal, Vol. 55, No. 1, pp. 42-50, July, 1988. Original article submitted March 2, 1987.

 0022-0841/88/5501-0730 $12.50

the problem, and the complexity of the algorithm when even simple models of turbulence are used, this assumption is adequate for the first stage of the investigation. The calculations are performed in a wide range of Re_{ef}. The theoretical velocity fields best agreeing with experiment are noted below.

At the boundaries of the given region, conditions for the components of the velocity vector are specified; the pressure at an arbitrary point is assumed to be zero, and the pressure is determined accurately in the volume, except for some additive constant.

It is convenient to write Eq. (1) in vectorial form in order to describe the algorithm for solution of the given problem

$$\Lambda f = 0, \quad f = \begin{bmatrix} u_1 \\ \vdots \\ u_N \\ P \end{bmatrix}, \quad \Lambda = \begin{bmatrix} L & 0 & \dots & \frac{\partial}{\partial x_1} \\ \dots & \dots & \dots & \dots \\ 0 & \dots & L & \frac{\partial}{\partial x_N} \\ \frac{\partial}{\partial x_1} & \dots & \frac{\partial}{\partial x_N} & 0 \end{bmatrix}, \tag{2}$$

$$L = \sum_{l=1}^{N} \left(u_l \frac{\partial}{\partial x_l} - \frac{1}{\mathrm{Re}_{ef}} \frac{\partial^2}{\partial x_l^2} \right).$$

The economic difference scheme constructed in [2, 3] on the basis of the fractional-step method is used. The solution is sought by the establishment method, setting the steady Navier–Stokes equations in correspondence with their nonsteady analogs, and the additional term $(1/A_p)(\partial P/\partial t)$ is introduced in the continuity equation

$$A \frac{\partial f}{\partial t} + \Lambda f = 0, \quad f|_{t=0} = f_0, \quad A = \begin{bmatrix} 1 & \dots & 0 & 0 \\ \dots & \dots & \dots & \dots \\ 0 & \dots & 1 & 0 \\ 0 & \dots & 0 & \frac{1}{A_P} \end{bmatrix}. \tag{3}$$

If $\Lambda^{(s)}$ is the difference matrix operator approximating the differential operator Λ with order s relative to the spatial step h, the difference analog of Eq. (3) may be the system

$$A \frac{f^{n+1} - f^n}{\tau} + \Lambda^{(s)} f^{n+1} = 0. \tag{4}$$

If Eq. (4) is to be linear, the operator $\Lambda^{(s)}$ must be taken at the n-th layer, here and below. For simplicity of notation, the superscript n is omitted.

The values of the components of the vector f^{n+1} at time t^{n+1} are found from their values at time t^n, i.e., $f^{n+1} = f^n + \xi^{n+1}$. Then it follows from Eq. (4) that

$$(E + \tau A^{-1} \Lambda^{(s)}) \xi = -\tau A^{-1} \Lambda^{(s)} f^n, \tag{5}$$

where E is a unit matrix and

$$\xi = \begin{bmatrix} \xi_{u_L} \\ \vdots \\ \xi_{u_N} \\ \xi_P \end{bmatrix}.$$

Resolving the operator $\Lambda_N^{(s)}$ with respect to the spatial variable: $\Lambda^{(s)} = \sum_{l=1}^{N} \Lambda_l^{(s)}$, where $\Lambda_\ell^{(s)}$ includes the approximations of all the derivatives with respect to x_ℓ, and implicit

scheme is constructed for the resolution of the problem in Eq. (5) with respect to N fractional steps

$$(E + \tau A^{-1}\Lambda_l^{(s)})\xi^{n+l/N} = \xi^{n+(l-1)/N},\ l = I,\ \ldots,\ N, \tag{6}$$

where $\xi^n = -\tau A^{-1}\Lambda^{(s)}f^n$.

Eliminating the intermediate fractional steps, a relation is obtained between f^{n+1} and f^n

$$\prod_{l=1}^{N}(E + \tau A^{-1}\Lambda_i^{(s)})\,\xi^{n+1} = \xi^n \quad \text{or}$$

$$A\frac{f^{n+1} - f^n}{\tau} + \Lambda^{(s)}f^{n+1} + (\tau A^{-1}(\Lambda_1^{(s)}\Lambda_2^{(s)} + \ldots) + (\tau A^{-1})^{N-1}\Lambda_1^{(s)}\ldots\Lambda_N^{(s)})(f^{n+1} - f^n) = 0. \tag{7}$$

Since $f^{n+1} - f^n \to 0$ on establishment, the solution of Eq. (6) tends to the solution $\Lambda^{(s)}f^{n+1} = 0$. Thus, the solution of the difference equations approximating the system of differential equations in Eq. (1) may be obtained with an error determined by the capabilities of the computer. In each fractional step, the system in Eq. (6) is solved by scalar fitting.

The choice of boundary conditions has a significant influence on the formation of the flow pattern in the calculation region. As shown by comparing the results of the calculations with experimental data, the "adhesion" condition $-\ V|_{boun} = 0$ – is natural for flow in channels of considerable length, where the friction at the wall has the determining influence on the formation of the velocity profile. However, in furnace chambers, the structure of the flow is determined by pulses introduced by high-speed jets and the thickness of the boundary layer is small in comparison with the chamber dimensions. Most of the energy is consumed in rearrangement of the flow and only a little of it in frictional losses at the walls. The turbulent viscosity, which changes little in the flow core, is sharply reduced close to the wall. Taking account of the need to apply a rough calculation grid, it may be concluded in this case that it is expedient to introduce "slipping" boundary conditions at the boundary surfaces, that is,

$$V_n|_\gamma = 0 \quad \text{and} \quad \left.\frac{\partial V_\tau}{\partial n}\right|_\gamma = 0.$$

Since it is of interest to calculate three-dimensional flows, and the surface γ may be oriented arbitrarily in space, the realization of "slipping" conditions is now considered in more detail. The first condition gives the equation

$$\sum_{l=1}^{N} u_l n_l = 0. \tag{8}$$

The second is equivalent to the system

$$\begin{bmatrix} 1 - n_1n_1 & -n_1n_2 & \ldots & -n_1n_N \\ \ldots & \ldots & \ldots & \ldots \\ -n_N n_1 & \ldots & \ldots & 1 - n_N n_N \end{bmatrix}\sigma\begin{bmatrix} u_1 \\ \vdots \\ u_N \end{bmatrix}_\gamma = 0, \tag{9}$$

where $\sigma = \sum_{P=1}^{N} n_P \frac{\partial}{\partial x_P}$ is a differential operator. When N = 3, this system of equations reduces to the simpler form

$$\begin{bmatrix} 1 - n_1n_1 & -n_1n_2 & -n_1n_3 \\ n_2 & -n_1 & 0 \\ n_3 & 0 & -n_1 \end{bmatrix}\sigma\begin{bmatrix} u_1 \\ u_2 \\ u_3 \end{bmatrix}_\gamma = 0. \tag{10}$$

Thus, four scalar equations for the three unknowns (u_1, u_2, u_3) are obtained from the boundary conditions. However, the components of the unit vector n are related as: $n_1^2 + n_2^2 + n_3^2 = 1$, and the determinant of Eq. (10) is zero, i.e., only two of the three equations may be used. Finally, it follows from Eqs. (8) and (10) that at the boundary γ

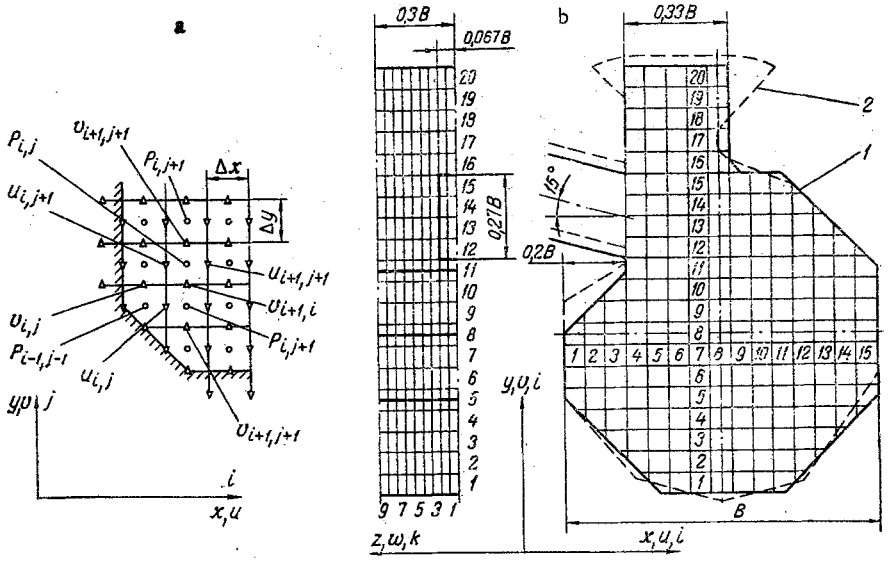

Fig. 1. Calculation grid: a) fragment of plane hybrid grid; b) comparison of geometry: 1) contours of mathematical model; 2) contours of physical model.

$$\begin{bmatrix} n_1 & n_2 & n_3 \\ n_2\sigma & -n_1\sigma & 0 \\ n_3\sigma & 0 & n_1\sigma \end{bmatrix} \begin{bmatrix} u_1 \\ u_2 \\ u_3 \end{bmatrix}_\nu = 0. \tag{11}$$

The system in Eq. (11) is simplified if one of the coordinate axes, for example, x_3, is directed parallel to the boundary surface. Then $n_3 = 0$ and $\Omega V = 0$

$$\Omega = \begin{bmatrix} n_1 & n_2 & 0 \\ n_2\sigma & -n_1\sigma & 0 \\ 0 & 0 & n_1\sigma \end{bmatrix}, \quad V = \begin{bmatrix} u_1 \\ u_2 \\ u_3 \end{bmatrix}_\nu.$$

In order to organize the iterative process, as in the case of Eq. (3), this system is set in correspondence with its nonsteady analog $\partial V/\partial t + \Omega V = 0$ and the operator Ω is written in the form: $\Omega = \Omega_1 + \Omega_2$, where

$$\Omega_1 = \begin{bmatrix} n_1 & 0 & 0 \\ 0 & -n_1\sigma & 0 \\ 0 & 0 & \dfrac{n_1\sigma}{2} \end{bmatrix}, \quad \Omega_2 = \begin{bmatrix} 0 & n_2 & 0 \\ n_2\sigma & 0 & 0 \\ 0 & 0 & \dfrac{n_1\sigma}{2} \end{bmatrix}.$$

In the odd (n + 1)-th time layer, the soluton of the following system is sought

$$\frac{V^{n+1} - V^n}{\tau} + \Omega_1 V^{n+1} + \Omega_2 V^n = 0, \tag{12a}$$

and in the even (n + 2)-th step

$$\frac{V^{n+2} - V^{n+1}}{\tau} + \Omega_1 V^{n+1} + \Omega_2 V^{n+2} = 0. \tag{12b}$$

In each of Eqs. (12a) and (12b), a scheme of resolution with respect to the directions similar to that in Eq. (6) is employed.

For transition from differential equations to finite-difference equations, the calculation region is covered by a hybrid grid. The coordinates x_1, x_2, x_3 are denoted by x, y, z, and the projections of the velocity vector u_1, u_2, u_3 by u, v, w, respectively. The cell structure of this grid for the plane case is shown in Fig. 1a. The pressure is determined

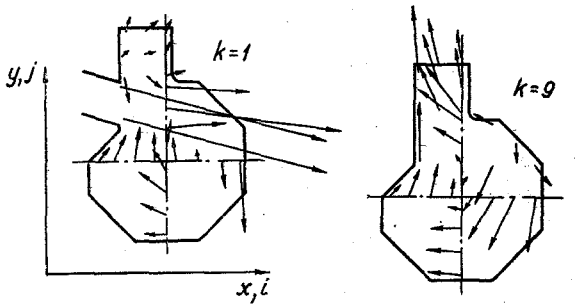

Fig. 2. Velocity fields in vortical furnace calculated in FOS, Re_{ef} = 500.

at the center of the cell $P_{i,j}$, relative to which the continuity equation is approximated. The projections of the momentum equation on the axes x and y is approximted by points u and v, respectively. The boundaries of the region parallel to the coordinate planes pass through the horizontal and vertical boundaries of the cell and the sloping boundaries through the velocity points, passing the points with the pressure. The partial derivatives in the continuity equation and the diffusional terms and pressure gradient are approximated on such a grid with second-order accuracy relative to the spatial step.

For the convective terms, approximations of two forms are used: first- and second-order accuracy. The first-order approximation is based on the well-known scheme with a donor cell [4] and the second-order approximation on a scheme with central differences [3].

The above method is used to calculate the isothermal aerodynamics of a vortex furnace of a small-scale E-500 boiler at the Novosibirsk heat and electric power plant TÉTs-3. This furnace is a complex object from the viewpoint of mathematical modeling. A vortex with a horizontal axis is created by two high-speed jets, which intersect. Therefore, only a three-dimensional model can be used for the calculations. Whereas a cylindrical coordinate system is preferable for the vortex, the chamber boundaries are best described in a Cartesian system. The flow is characterized by very large velocity-field gradients.

Part of the furnace volume enclosed between the axial planes of the furnace and the burner is isolated for the calculation (Fig. 1b). The x axis of the Cartesian coordinate system is perpendicular to the front from the burner to the rear wall, the y axis vertically upward, and the z axis parallel to the front of the boiler. The corresponding dimensions along these directions are: B = 1, H = 1.33, S = 0.3; and the number of grid points is: N1 × N2 × N3 = 15 × 20 × 9.

Thus, $\Delta x = \Delta y = 1/15$ and $\Delta z = 1/30$. The depth of the furnace chamber is taken as the normalizing dimension and the velocity at the burner outlet as the normalizing velocity. The calculation region includes half the burner. Its area is 8 cells, in which the projections of the input velocity are specified: $U_{in} = 1.0$; $V_{in} = 0.267$ (the angle of slope of the burner is 15°). The ratio of the total area of the inputs to the cross-sectional area of the combustion chamber $\Sigma f/F_0 = 0.058$. The "slipping" condition is imposed at all the surfaces parallel to the z axis and the symmetry condition at all the normal planes. The output diffusor connecting the combustion and precombustion chambers is replaced by a straight channel, at the free boundary of which "soft" [4] boundary conditions are specified.

Calculations are performed in a first-order scheme (FOS) with Re_{ef} = 30, 100, 200, 500, 1000 and in a second-order scheme (SOS) with Re_{ef} = 200 and 500. When using FOS, Re_{ef} has considerable influence on the character of the flow in the range 30-100. When $100 < Re_{ef} < 500$, this influence is markedly reduced; it vanishes when $Re_{ef} > 500$. When $Re_{ef} = 30$, the flow leaving the burner is twisted and, passing the combustion chamber, it is directed toward the contraction. There is practically no vortical flow in the chamber. With increase in Re_{ef}, the swirling in the chamber increases: On the one hand, the jet becomes longer-range; on the other, it ejects a larger quantity of gas from the furnace volume. However, even when $Re_{ef} = 500$, the multiplicity of circulation K, equal to the ratio of the gas flow rate passing through the radial cross section to the flow rate at the chamber input, is no greater than 1. The velocity field for this case in the burner

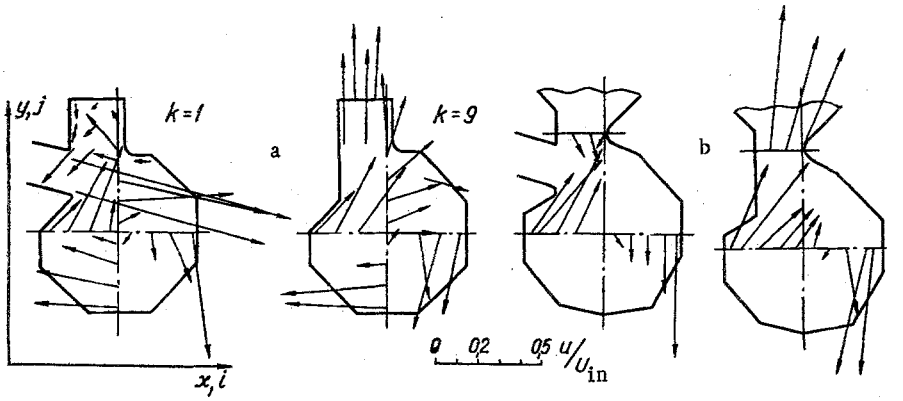

Fig. 3. Comparison of theoretical and experimental velocity fields: a) FOS calculation, Re_{ef} = 500; b) isothermal blowing in model.

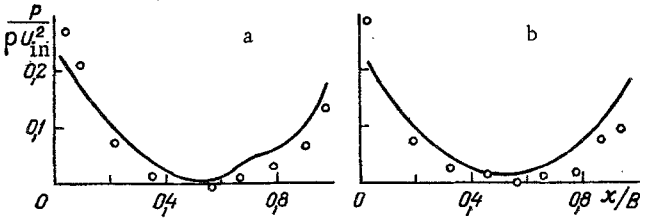

Fig. 4. Distribution of dimensionless static pressure along horizontal diameter: a) in burner cross section, k = 1; b) in axial cross section of furnace, k = 9; the curves correspond to calculation and the points to experiment.

cross section (k = 1) and in the axial cross section of the furnace is shown in Fig. 2. They are distinguished by strong shift toward the rear wall of the center of the vortex when k = 1, small velocity-field gradients, and small velocity-retention coefficient ε [5]. At the rear wall, ε = 0.35. It is noteworthy that the flow leaving the burner reaches the opposite wall and is partially deflected to the lower part of the furnace, partially turned in the horizontal plane in the opposite direction. Therefore, in the axial cross section (k = 9), there is no recirculation of the gas, and the whole flow from the lower part of the chamber is directed to the output window. In conclusion, it may be noted that the velocity fields which may be obtained using FOS correspond to more viscous flow than that observed in physical models. This is explained by the presence of schematic viscosity in FOS [6] or, in other words, insufficient accuracy of the approximation of convective terms. The schematic viscosity accompanying FOS corresponds to Re ≈ 100 in the present problem. Correspondingly, the increase in Re_{ef} by an order of magnitude – from 100 to 1000 – does not lead to significant change in the velocity fields calculated in FOS. Hence, calculation of the aerodynamics of such furnaces must be based on schemes of higher order.

A central-difference approximation of the convective terms is used here to obtain the SOS. The SOS calculations assume Re_{ef} = 200 and 500. Note that even in this range Re_{ef} is one of the factors determining the flow pattern. It is an empirical constant which offers the possibility of establishing the relation between calculation and experiment. The results of SOS calculations for Re_{ef} = 500 are shown in Fig. 3a. The level of tangential velocity here is 2.5 times greater than when using FOS. Vortical flow is seen over the whole volume; turning of the flow in the horizontal plane of the cross section is not seen. The multiplicity of the circulation is K = 2.5.

In Fig. 3b, for comparison, the results of isothermal injection of the vortical furnace of the E-500 boiler at the Novosibirsk heat and electrical power station TÉTs-3 are shown, and in Fig. 4 the distribution of the dimensionless static pressure (normalized with respect to ρU_{in}) along the chamber diameter is shown. The theoretical and experimental (obtained by V. F. Litvinenko at the Scientific Design Department, I. I. Polzunov Central Scientific-

Research Institute for the Planning and Design of Boilers and Turbines) fields are in good agreement. Active vortical motion is observed in both the mathematical and physical models, with a maximum tangential velocity at the rear wall of ~0.65 U_{in}. The identical position of the center of the vortex is noteworthy: In the burner cross section, it coincides with the geometric center of the chamber; between the burners it is shifted by 0.1 B to the right. The flow output in both cases is between the burners, above which downward flow is seen. In Fig. 3a, rarrangement of the flow characteristic of vortical chambers is shown. Whereas at the rear wall a narrower velocity profile is seen in the burner cross section and a somewhat trucated profile in the axial cross section of the chamber, the tangential velocity gradient between the burners is higher than that below them in the hearth.

The drag coefficient of the combustion chamber, equal to the ratio of the difference in mean total pressure head at the chamber inlet and the outlet from the neck to the dynamic pressure head in the burner, is determined from the calculated velocity fields and pressures. It is 0.856. Data on the drag are in satisfactory agreement with the experimental results in [5], where the relative loss in total pressure head from the aperture to the output cross section of the cooling chamber is around 1.1. The explanation for the greater experimental than theoretical values may be that the energy losses in the cooling chamber do not appear in the theoretical values, since the cooling chamber is not included in the mathematical model.

Thus, the proposed method allows data to be obtained by means of calculation on the aerodynamics of three-dimensional flows, the flow structure of which is determined by the momenta of the incoming jets.

NOTATION

x_1, x_2, x_3 or x, y, z, Cartesian coordinates; u_1, u_2, u_3 or u, v, w, the corresponding components of the velocity vector; P, pressure normalized with respect to ρU_0^2; Re_{ef}, Reynolds number calculated from the effective viscosity; Λ, differential matrix operator; L, differential operator taking account of convective and viscous terms; A_p, weighting factor for $\partial P/\partial t$; h, τ, spatial and time steps; s, order of approximation; ξ, correction vector; n, unit normal to surface with coordinates n_1, n_2, n_3; V_n, V_τ, components of velocity vector V normal and tangential to surface γ; Ω, differential matrix operator of boundary conditions; i, j, k, subscripts corresponding to coordinates x, y, z; K, multiplicity of circulation; ε, velocity retention coefficient.

LITERATURE CITED

1. V. O. Krol', "Numerical modeling of aerodynamics and combustion in annular furnace chambers," Author's Abstract of Candidate's Dissertation, Alma-Ata (1985).
2. S. B. Koleshko, in: Numerical Methods of Continuum Mechanics [in Russian], Vol. 10, Novosibirsk (1979), No. 3, pp. 100-105.
3. Yu. É. Egorov and S. B. Koleshko, in: Dynamics of Inhomogeneous and Compressible Media [in Russian], N. N. Polyakhov (ed.), Leningrad (1984), pp. 80-92.
4. P. J. Roache, Computation Hydrodynamics, McGraw-Hill (1960).
5. N. V. Golovanov, A. A. Popov, and V. F. Litvinenko, Tr. TsKTI, No. 161, 50-55 (1978).
6. S. Patankar, Numerical Methods of Solving Problems of the Heat Transfer and Dynamics of Liquids [Russian translation], Moscow (1984).